

Ceramic toughness assessment through edge chipping measurements—Influence of interfacial friction

F. Petit*, V. Vandeneede, F. Cambier

Belgian Ceramic Research Centre, 4 Avenue du Gouverneur Cornez, B-7000 Mons, Belgium

Received 28 October 2008; received in revised form 8 January 2009; accepted 14 January 2009

Available online 12 February 2009

Abstract

In this paper, a comparative study between two techniques to determine material toughness through edge chipping measurements, is presented. The first technique relies on static Rockwell indentations, performed at well-defined distances from the edge with an increasing load until chipping occurs. The second technique keeps the applied load constant but drives the Rockwell indenter towards the edge at constant speed until a chip is formed (scratch testing). In most studied cases, our experimental results on ceramics are shown to conform with the predictions of previous models in the literature expressing the toughness K_{Ic} as a function of chip size l_c and critical chipping load P through $K_{Ic} \cong P/l_c^{3/2}$. However, for silicon carbide, the toughness values obtained by both variants of the method are mutually incompatible. The discrepancy is shown to be related to the tangential loading occurring during scratch testing. A new equation for toughness assessment is derived that takes into account the influence of friction. This equation is demonstrated to match well the experimental results both for static and sliding indentation.

© 2009 Elsevier Ltd. All rights reserved.

Keywords: Ceramics; Cracking; Scratch test; Friction; Edge chipping

1. Introduction

It has long been recognised that edge chipping resistance can be easily determined by indentation techniques.¹ Basically, the technique consists in performing an indentation near the edge of a specimen with increasing applied load until a flake forms. The mechanism of the chip formation is understood as follows: during indentation, a median/radial system of cracks forms in the material sub-surface. As the load increases, these cracks tend to grow rapidly towards the free edge. Finally, when they reach the sample edge, a chip detaches from the specimen.

Several papers have pointed out the existence of a bi-unique relation between the flaking load P and the chip size l_c ^{3–9} (Fig. 1). Usually, experimental data scatter do not allow to determine the exact relationship between P and l_c and therefore a linear dependency $P \cong l_c$ between both quantities is assumed. However, a recent approach from Chai and Lawn² has pointed out that the actual dependency would be $P \cong l_c^{3/2}$. The latter relation was derived by using sound fracture mechanics instead of empirical

evidence.³ In Ref. [2] the authors considered the stress intensity factor generated by a sharp indenter on a median crack located at some distance from the edge. They show that at equilibrium when the stress intensity factor equals the toughness, the critical load for chipping takes the form:

$$\frac{P}{l_c^{3/2}} = \left(\frac{K_c}{\chi_e}\right) \left(\frac{c_F}{l_c}\right)^{3/2} f\left(\frac{c_F}{l_c}\right) = \beta K_c \quad (1)$$

where K_c is the material toughness, c_F the depth of the crack when it becomes unstable, χ_e an indentation coefficient relating to the elastic component of the indentation field and $f(c_F/l_c)$ a dimensionless and material-independent function.

Eq. (1) demonstrates the possibility of assessing toughness through simple edge chipping measurements. The validity of this relation was confirmed by testing several ceramics through edge chipping measurements performed by Vickers indentations. A value of $\beta = 9.3 \pm 1.3$ was derived from direct measurements on glass.

An obvious limitation of Eq. (1) is the assumption that the contact between the indenter and the material is frictionless. Although, we may assume that friction can be neglected in the “static” configuration test (e.g., the usual indentation test where

* Corresponding author. Tel.: +32 65 40 34 64; fax: +32 65 40 34 60.
E-mail address: f.petit@brc.be (F. Petit).

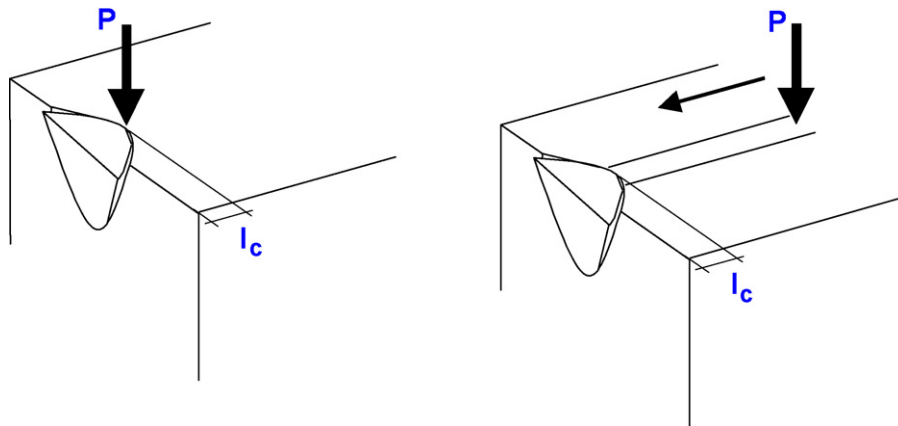


Fig. 1. Schematic drawings illustrating static (left) and sliding (right) edge toughness measurements.

the material is loaded by a normal force only), it is obviously not the case in a scratch test experiment where the tangential loading component will likely influence the crack path and the critical chipping load.

Through experiments conducted on a broad set of brittle ceramic materials, we demonstrate the validity of this statement. A direct application of the Chai and Lawn model² shows a significant discrepancy between toughness assessments obtained by both configuration testing. A modification of the original Chai and Lawn equation to incorporate the influence of friction is therefore proposed allowing to get a better agreement between both techniques.

2. Experimental procedure—materials and sample preparation

In this study, a set of five different technical ceramics was used. The materials were chosen to span a broad range of toughness (K_{Ic}). The whole set includes two different aluminas (referred hereafter to as alumina A—99.9% purity and alumina B—98% purity), two different yttria stabilized zirconias (referred to as zirconia A and B hereafter) and one silicon carbide. All these grades have a commercial origin.

Prior to characterisation, 4 mm × 3 mm × 45 mm bars were cut from the as-received ceramic blocks, machined to become ground flat and polished with diamond paste down to a 3- μ m finish. A small notch of nearly 1 mm deep was machined in half of the bars for subsequent toughness (K_{Ic}) characterisation. K_{Ic} was determined using the single edge V-notched beam – SEVNB – technique^{10,11} using a three-point bending test apparatus (15 mm span) and a universal testing machine (Z-100 Universal testing machine—Zwick, Germany). The crosshead speed was kept constant at 0.1 mm/min. At least of five different measurements were realized to obtain accurate toughness measurements.

Edge chipping measurements were performed on rectangular blocks of about 30 mm × 15 mm × 4 mm. The top face of these samples was polished as above. Great care was taken to keep right angle sharp edges of samples all along the machining/polishing steps.

Static indentations measurements were performed using an universal testing machine equipped with a purpose-built-in

device. This device had two components: a holder for clamping the specimen and an indenter fixed on the crosshead of the machine. The static indentations were realized according to the following procedure: first, the specimen was placed in the holder fixed on an X–Y table equipped with micrometric screws. Using the screws, the sample was moved to a position where the edge and the indenter tip are aligned. Then the table was moved for displacing the indenter at a prescribed distance from the edge. For these tests, the loading rate was 0.1 mm/min. Complete unloading was realized immediately upon chip formation whenever this was recorded by the machine. Rupture was considered to occur after a 20% force decrease. Several indentations could be realized on a single specimen edge providing a significant distance (at least 2 mm) between consecutive chips was respected in order to avoid crack overlap.

Sliding indentations measurements were performed using a REVETEST scratch tester (CSM Instruments—Switzerland). In this work, test pieces identical to those machined for static measurements were used. The specimens were clamped in the holder of a motorized X–Y table allowing sample motions right below the indenter. Experiments were carried out considering several displacement speeds (0.5 mm/min, 5 mm/min and 15 mm/min) and loads (20 N, 40 N, 60 N and 80 N). These loads were chosen low enough to prevent spalling and/or lateral crack formation during scratching. All scratches were performed perpendicularly to the edges and unloading occurred upon chip formation detected by a corresponding peak of acoustic emission.

For sliding as well as for static indentations, the actual chip size l_c was estimated through measurements of the scar remnant on the sample by using an optical microscope (Fig. 1).

All indentations were realized using a Rockwell diamond C indenter (tip radius of 0.2 mm) whose integrity was verified between each series of indentations.

3. Results

Data of conventional toughness measurements are given in Table 1. Zirconias are clearly the most resistant materials of the study followed by the aluminas and silicon carbide.

Table 1
Materials toughness (SEVNB measurements).

Grade	K_{Ic} (MPa m ^{1/2})
Zirconia A	7.1
Zirconia B	12.0
Alumina A	4.1
Alumina B	3.5
SiC	3.2

Fig. 2 exhibits the results of edge chipping measurements. The chipping load is plotted as a function of the flake size l_c measured by microscopy.

Examination of these results confirms that the flake length and the fracture load are related to each other. Higher fracture loads are required to form larger chips, as expected.

For zirconias, the results obtained by static indentation and scratch testing demonstrate very similar behaviours: the combination of the two series of points suggests the existence of a unique non-linear dependency between the chip size and the applied load. For alumina, such a trend is less obvious. For instance in case of alumina A, a shift between the two series of points can be noticed in the flake length range between 0.2 mm

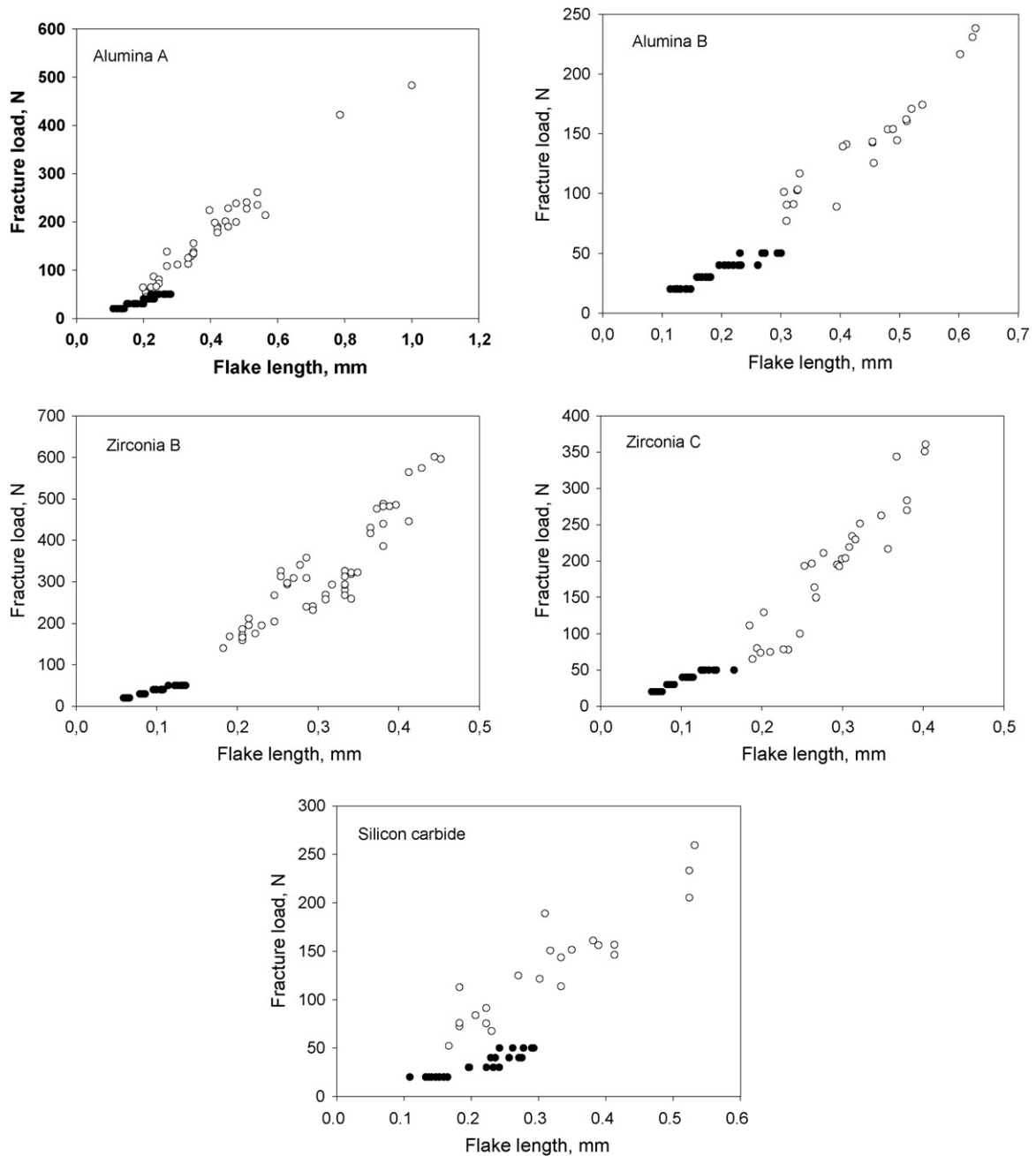


Fig. 2. Results of edge chipping measurements (uncorrected values).

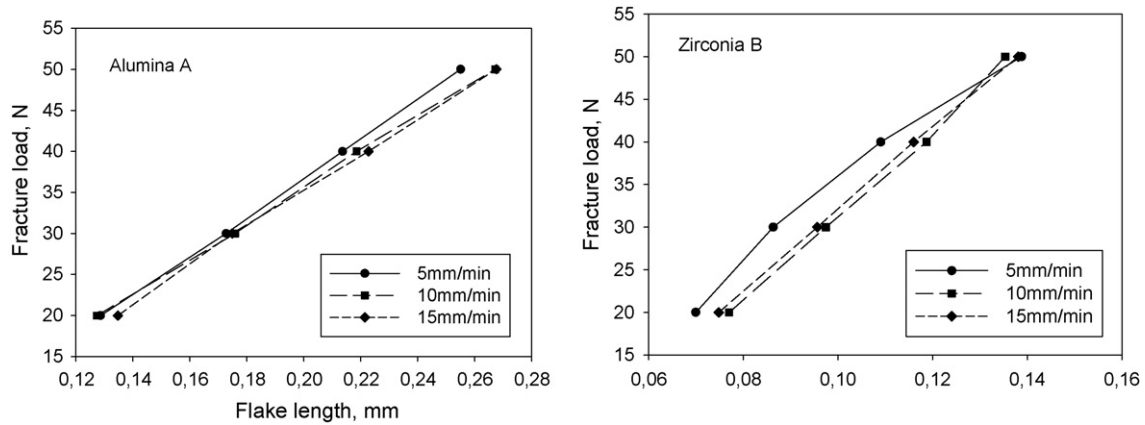


Fig. 3. Influence of the sliding speed on the flaking load (illustrated in the case of alumina A and zirconia B).

and 0.3 mm. The shift is even more pronounced in case of silicon carbide. For this material, the critical loads determined through scratch testing are almost three times lower than those measured by static indentation for similar flake length.

The experimental scattering seems essentially to be materials dependent. It is quite significant for static indentation measurements and slightly lower for scratch testing. The scatter can be partly explained by some variations of flake geometry which makes chip size measurement uncertain. When distorted chip geometries are observed, they present a larger surface of rupture than the “ideal” flake geometry pictured in Fig. 1. In those cases, higher loads than those needed to form a chip with a more regular geometry are probably required. As a consequence, the comparison of chip sizes can sometimes be put into question. In some cases, reorientations of the crack path before the chip formation have also been observed. Usually, those cracks tend to run parallel to the edge before intercepting it. Those reorientations suggest a branching phenomenon occurring when the main crack hits a local interacting flaw (porosity, local anisotropy or heterogeneity, etc.). In some cases, the crack stops before reaching the free edge (especially in very tough materials like zirconias). Finally, some shape distortions might also be related to the grinding processes through the introduction of sub-surface flaws. In any case, no obvious correlation between the flake shape and microstructures was found. Influence of specimen roughness was however not investigated in the present study.

Scratches observed by optical microscopy show that cracks are present all along the wake (without noticeable lateral chipping). No evidence of significant plastic grooving was detected along the scratches. However, the presence of plastic remnant imprints at the edge of some scars may suggest that the fracture process is driven by an elastic/plastic stress field. The cracks observed along the scratches are typically partial ring cracks that deviate close to the edge to propagate in a half-cone shape as for static indentation. This change can probably be related to the change in stress field in front of the indenter close to the free edge. A half-cone fracture is then initiated leading to the chip formation.

Contrarily to the “static” indentation experiments, distortions of chips are negligible in case of scratch testing. This can

be related to the fact that chips are smaller (due to the lower applied loads) and therefore less sensitive to the influence of neighbouring flaws during propagation.

4. Influence of friction in the chipping mechanism and material toughness assessment

To explain the discrepancy between “static” and “sliding” experiments, the influence of the displacement speed during scratching was investigated as well as that of friction. During a scratch test, friction is known to generate an asymmetrical stress field involving an in-plane tensile stress behind the indenter and an in-plane compressive stress in front of it. Consequently, as the peak tensile stress increases in presence of friction, the critical cracking load should decrease correlatively.

By performing scratch tests at different velocities (5 mm/min, 10 mm/min and 15 mm/min), it was easily checked that the scratch velocity exerts almost no influence on chipping (Fig. 3).

Experimental measurements of friction were carried out on alumina A, zirconia B and silicon carbide by performing complementary scratch tests. A constant normal force of 30 N was used to prevent cracking and three different velocities were still considered, i.e., 5 mm/min, 10 mm/min and 15 mm/min. The results of three different scratches are presented in Fig. 4.

The average friction coefficient was calculated to be 0.10, 0.14 and 0.27 for zirconia B, alumina A and silicon carbide, respectively.

To get a quantitative insight on the effect of friction on chipping, it is necessary to consider some elementary fracture mechanics. The stress intensity K for a semi-circular flaw of depth c in a monolithic material subjected to a uniform, i.e., depth-independent tensile stress σ is

$$K \cong \chi \sigma \sqrt{c} \quad (2)$$

where χ is a constant.

In case where the tensile stress is generated by a contact with an indenter loaded at force P , simple dimensional analysis provides $\sigma \cong \alpha P/c^2$ where α is a dimensionless constant. Therefore,

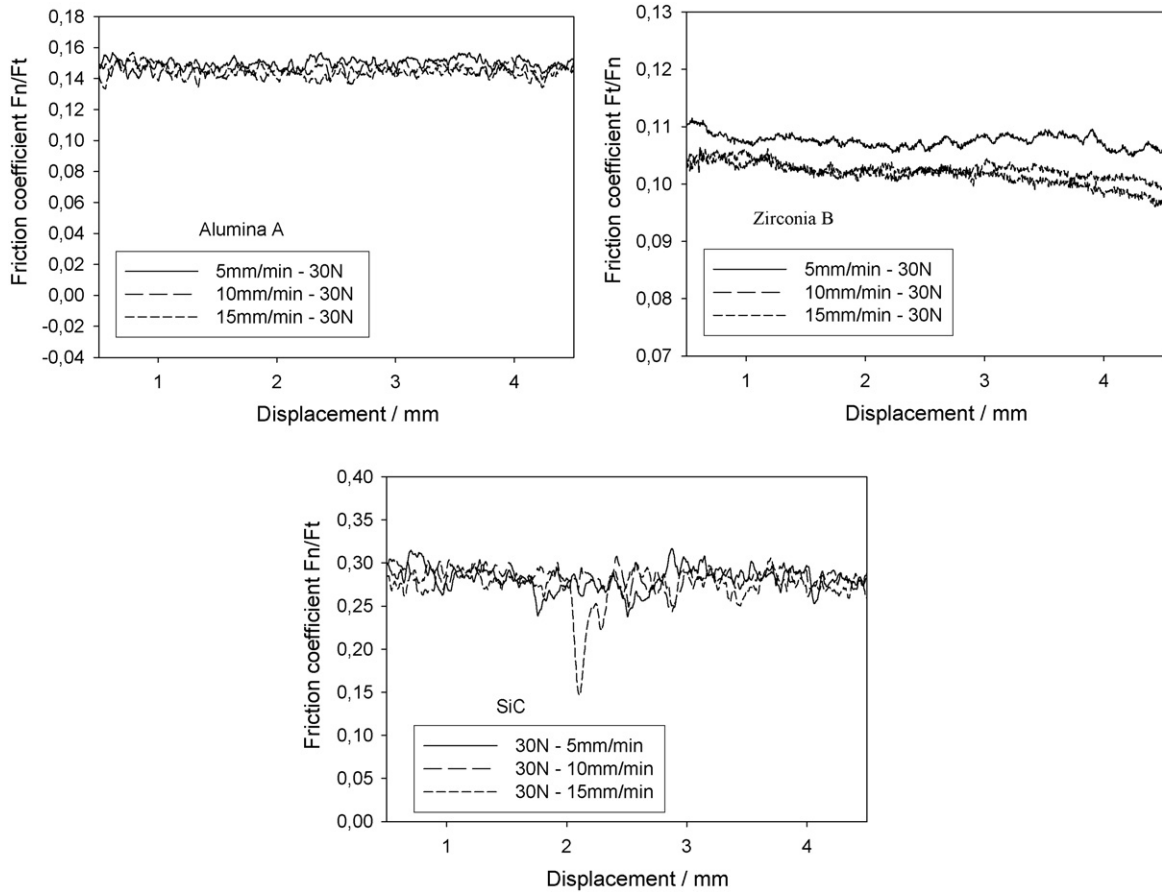


Fig. 4. Friction coefficients measured at different scratching velocities.

the stress intensity factor takes the usual form:

$$K \cong \alpha \chi \frac{P}{c^{3/2}} = \chi_e \frac{P}{c^{3/2}} \quad (3)$$

with $\chi_e = \alpha \chi$.

The condition of cracking is obtained when $K = K_c$ with K_c the material toughness.

For edge chipping, Chai and Lawn have proposed to accommodate the influence of the front free surface which begins to be felt when the crack propagates by normalizing crack size c relative to indent location l_c . They have demonstrated that the condition $K = K_c$ with K given by Eq. (3) turns out to be

$$K_c \cong \chi_e \left[\left(\frac{c_F}{l_c} \right)^{-3/2} \frac{1}{f(c_F/l_c)} \right] \frac{P_c}{l_c^{3/2}} = \frac{1}{\beta} \frac{P_c}{l_c^{3/2}} \quad (4)$$

where $1/\beta = \chi_e [(c_F/l_c)^{-3/2} 1/f(c_F/l_c)]$, c_F is the crack critical size when it becomes unstable and $f(c_F/l_c)$ is a constant, independent of material.

Eq. (4) was derived by neglecting any crack size dependence on K_c and by assuming that the indenter does not unload prior to chipping in order to neglect any residual inelastic component in the stress field.

Although Eq. (4) exhibits dependency between toughness, cracking load and chip size, an obvious limitation of this expres-

sion is that it does not include the influence of friction which cannot be neglected during scratching. It is however straightforward to modify Eq. (4) in order to accommodate friction in a reasonable way.

In case of a sliding spherical asperity, the maximum of the tensile stress will occur at the trailing edge of the stylus. This stress will cause the material to fracture. The corresponding stress intensity is classically given by¹²

$$K \cong \chi \sigma \left(1 + \frac{3(4 + \nu)}{8(1 - 2\nu)} \pi \mu \right) \sqrt{c} \quad (5)$$

where μ and ν are the friction coefficient and the Poisson's coefficient, respectively. Based on Eq. (5), it is possible to write an equivalent counterpart of the frictionless case described by Eq. (3)

$$K \cong \chi_e \left(1 + \frac{3(4 + \nu)}{8(1 - 2\nu)} \pi \mu \right) \frac{P}{c^{3/2}} \quad (6)$$

For $\mu = 0$, Eq. (6) becomes identical to Eq. (3).

Following Chai and Lawn² and normalizing crack size c relative to indent location l_c , the condition of cracking in presence

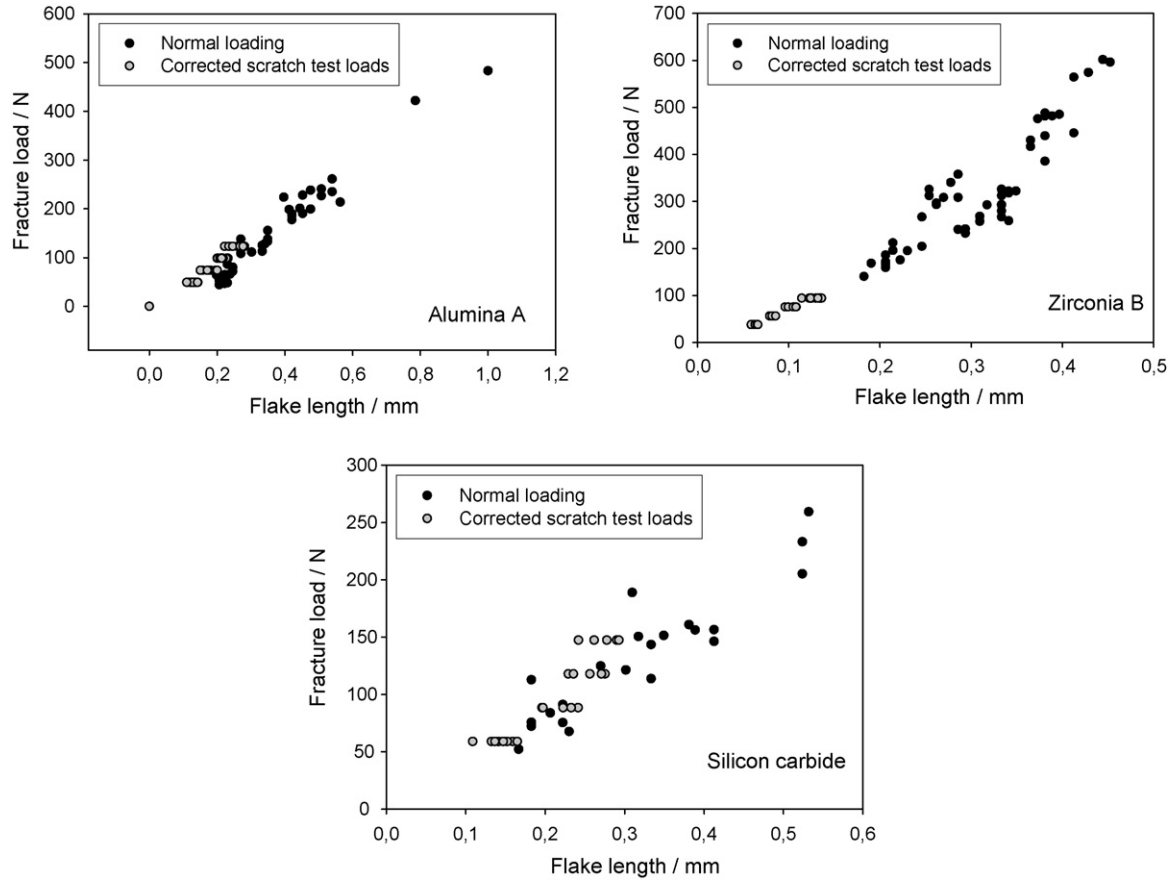


Fig. 5. Effect of the incorporation of friction in the critical loads measured by scratch testing (mean friction coefficients of 0.15, 0.11 and 0.27 were deduced for alumina A, zirconia B and silicon carbide, respectively).

of friction becomes

$$K_c \cong \chi_e \left[\left(\frac{c_F}{l_c} \right)^{-3/2} \frac{1}{f(c_F/l_c)} \right] \left(1 + \frac{3(4 + \nu)}{8(1 - 2\nu)} \pi \mu \right) \frac{P_c}{l_c^{3/2}}$$

$$= \frac{1}{\beta} \left(1 + \frac{3(4 + \nu)}{8(1 - 2\nu)} \pi \mu \right) \frac{P_c}{l_c^{3/2}} \quad (7)$$

Eq. (7) suggests that toughness can be correctly assessed only if the friction coefficient value is known. Comparison of Eqs. (4) and (7) shows that the critical chipping load in presence of friction is related to that of the frictionless case through:

$$P_{c,\mu} = P_c \frac{1}{1 + (3(4 + \nu)/8(1 - 2\nu))\pi\mu} \quad (8)$$

Therefore, if μ increases the critical chipping load decreases. To more clearly illustrate the influence of friction on the chipping load, the values obtained by scratch testing have been corrected using Eq. (8) and compared again with the values obtained by static indentation. The result of this correction is illustrated in Fig. 5 for alumina A, zirconia B and silicon carbide (other materials of the study behave similarly).

It is worth noticing that the proposed correction allows getting a much better correlation between both series of points. The agreement is now excellent even for alumina A and silicon carbide.

A plot of the critical load (incorporating the values obtained by normal loading and the corrected scratch test values) versus the chip size is given in Fig. 6 for each material. Regression fits of Eq. (5) with force-fit slopes 1.5 allow to determine values of the constant β .

Based on our experimental measurements, an average value of $\beta \cong 5.4$ was found. It can be noticed that this value differs from that found previously by Chai and Lawn ($\beta \cong 9.3$). The reason is probably that we used Rockwell indentation rather

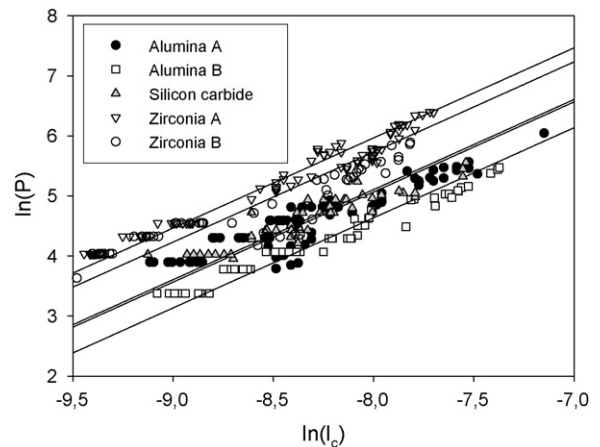


Fig. 6. Plot of chipping load P versus chip size l_c .

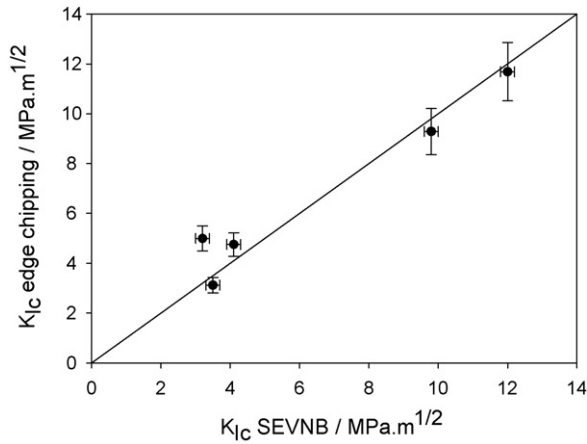


Fig. 7. Plot of SEVNB toughness versus values determined through edge chipping measurements.

than Vickers indentation as they did. With the value found, the material toughnesses were recalculated and compared with the SEVNB values. The result shown in Fig. 7 illustrates the rather good agreement between both methods by using Eq. (7).

5. Conclusions

In this study, static and sliding indentation have been used to assess the edge chipping resistance and the toughness of five different ceramics. The influence of the scratching speed was shown to be negligible in the chip formation for all studied materials. However, the influence of the friction coefficient was shown to exert a dramatic influence. Without considering friction, the chipping loads measured by scratch testing are not consistent with those derived from static measurements. Inspired from a recently published work by Chai and Lawn, a relation has been proposed to tackle the influence of friction. It is demonstrated that this new relation can fully explain all experimental results. Moreover, a good agreement between the toughness values determined through edge chipping measurements (either through static measurements of scratch testing) and SEVNB values is obtained.

Acknowledgement

The financial support of the Belgian SPF economy under the frame of contract No. CC CIF 957 is gratefully acknowledged.

References

- McCormick, N. J., Edge flaking as a measure of material performance. *Metals and Materials*, 1982, **8**, 154–157.
- Chai, H. and Lawn, B. R., A universal relation for edge chipping from sharp contacts in brittle materials: a simple means of toughness evaluation. *Acta Materialia*, 2007, **55**(7), 2555–2561.
- Petit, F., Descamps, P., Erauw, J. P. and Cambier, F., Toughness (K_{Ic}) measurement by a sliding indentation method. *Key Engineering Materials*, 2002, **206–213**, 629–632.
- Danzer, R., Hangl, M. and Paar, R., Edge chipping of brittle materials. In *Fractography of glasses and ceramics I*, ed. J. R. Varner and G. D. Quinn. *Ceramic transactions*, vol. 122. American Ceramic Society, Westerville (OH), 2001, pp. 43–56.
- Morrell, R. and Grant, A. J., Edge chipping of hard materials. *International Journal of Refractory Metals & Hard Materials*, 2001, **19**, 293–301.
- Paar, R., Hangl, M. and Danzer, R., Edge toughness of advanced ceramics. In *ECERS—European Ceramic Society fourth conference*, 1995.
- Gogotsi, G. A. and Mudrik, S. P., Fracture resistance of ceramics upon edge chipping. *Strength of Materials*, 2004, **36**(5), 545–547.
- Quinn, J., Su, L., Flanders, L. and Lloyd, I., Edge toughness and material properties related to the machining of dental ceramics. *Machining Science and Technology*, 2000, **4**(2), 291–304.
- Scieszka, S. F., Edge failure as a means of concurrently estimating the abrasion and edge fracture resistance of hard-metals. *Tribology International*, 2005, **38**, 834–842.
- Kübler, J., Fracture toughness of ceramics using the SEVNB method: from a preliminary study to a test method. In *Fracture Resistance Testing of Monolithic and Composite Brittle Materials*, ASTM STP 1409, ed. J. Salem, G. Quinn and Jenkins. ASTM International, West Conshohocken, PA, USA, 2002. p. 93–106.
- Damani, R., Gstrein, R. and Danzer, R., Critical notch-root radius effect in SENB-S fracture toughness testing. *Journal of the European Ceramic Society*, 1996, **16**, 695–702.
- Hamilton, G. M., Explicit equations for the stresses beneath a sliding spherical contact. In: Proceedings of the Instm. (National inter-university consortium for the science and technology of materials). *Mechanical Engineering C*, 197, 1983, 53–59.